Separation Science and Technology
Publication details, including instructions for authors and subscription information:
http://www.informaworld.com/smpp/title~content=t713708471

Adsorption Characteristics of Benzaldehyde, Sulphanilic acid, and p-Phenolsulfonate from Water, Acid, or Base Solutions onto Activated Carbon Cloth

Osman Duman[a]; Erol Ayranci[a]
[a] Department of Chemistry, Akdeniz University, Antalya, Turkey

To cite this Article Duman, Osman and Ayranci, Erol(2006) 'Adsorption Characteristics of Benzaldehyde, Sulphanilic acid, and p-Phenolsulfonate from Water, Acid, or Base Solutions onto Activated Carbon Cloth', Separation Science and Technology, 41: 16, 3673 — 3692
To link to this Article: DOI: 10.1080/01496390600915072
URL: http://dx.doi.org/10.1080/01496390600915072

Separation Science and Technology, 41: 3673–3692, 2006

ISSN 0149-6395 print/1520-5754 online
DOI: 10.1080/01496390600915072

Adsorption Characteristics of Benzaldehyde, Sulphanilic acid, and p-Phenolsulfonate from Water, Acid, or Base Solutions onto Activated Carbon Cloth

Osman Duman and Erol Ayranci
Department of Chemistry, Akdeniz University, Antalya, Turkey

Abstract: Adsorption of benzaldehyde (BA), sulphanilic acid (SA), and sodium salt of p-phenolsulfonic acid (p-PhS) from water, acid, or base solutions onto activated carbon cloth (ACC) was studied by in-situ UV-spectrophotometric method. Kinetics of adsorption was followed over 90 min and the data were fitted to first order rate law. The order of rate of adsorption was found to be BA $>$ SA $\approx$ p-PhS in water, BA $>$ p-PhS $>$ SA in 1 M H_2SO_4 and BA $>$ SA $>>$ p-PhS in 0.1 M NaOH. Competitive adsorptions of BA and SA from an equimolar mixture in 1 M H_2SO_4 and of BA and p-PhS from an equimolar mixture in H_2O were studied for exploring the possibilities of separation of binary mixtures. It was found that p-PhS was not adsorbed at all from 0.1 M NaOH solution. Adsorption isotherms of BA, SA, and p-PhS at 30°C were derived and the data were fitted to the Langmuir and Freundlich models. The Freundlich model was found to represent the experimental data better than the Langmuir model.

Keywords: Adsorption, competitive adsorption, activated carbon cloth, benzaldehyde, sulphanilic acid, p-phenolsulfonate

INTRODUCTION

The most important use of benzaldehyde is in organic synthesis, where it is the raw material for a large number of products. In this regard, a considerable amount of benzaldehyde is utilized to produce various aldehydes, such as

Received 3 May 2006, Accepted 22 June 2006
Address correspondence to Erol Ayranci, Department of Chemistry, Akdeniz University, Antalya 07058, Turkey. Tel.: (90) (242) 310 23 15; Fax: (90) (242) 227 89 11; E-mail: eayranci@akdeniz.edu.tr

cinnamic, methylcinnamic, amylcinnamic, and hexylcinnamic. Benzaldehyde is also used in the preparation of certain aniline dyes and of other products, including perfumes and flavorings. Sulphanilic acid is used in making azo dyes, pharmaceutical, and perfumery industry (1).

The adsorption capacity of an activated carbon depends on:

i. the nature of the adsorbent (e.g. functional groups present, specific surface area, and pore size distribution);
ii. the nature of adsorbate (e.g. functional groups present, polarity, hydrophobicity, molecular weight and size, solubility and pK_a or pK_b for weak acids or bases); and
iii. solution conditions (e.g. pH, temperature and adsorbate concentration, presence of competitive solutes, polarity of solvent).

Since many of the pollutants are weak acids or bases, the central fundamental issue is how to account simultaneously for the well documented importance of the pH of the aqueous solution and the surface chemistry of the adsorbent in adsorption (2).

The adsorbents having both a large adsorption capacity and adsorption rate are preferable. Activated carbon is such an adsorbent and widely used both in research and in practical applications. Activated carbon has three forms; granular, powder, and fiber or cloth. Activated carbon cloth or fiber has several unique characteristics compared with conventionally used granular or powder activated carbons. These materials are composed of thin fibers of the order of ten microns in diameters leading to greater adsorption rates, and hence contributing to the minimization of the reactor size. The cloth or fiber form of activated carbon also makes the handling of adsorbents much easier. Activated carbon cloth or fiber is produced from various raw materials such as polyacrilonitrile, rayon, cellulose, phenolic resins, and coal tar pitch (3–5).

The total porosity is classified into three groups by the International Union of Pure and Applied Chemistry (IUPAC). Micropores are defined as pores of a width not exceeding 20 Å, mesopores are pores of a width between 20 and 500 Å and macropores represent pores of a width greater than 500 Å (6, 7). Micropores have a significant effect in the adsorption of small solute molecules. Larger molecules are excluded from micropores but may be adsorbed into some or all of the mesopores, and all the macropores (8).

Recently, activated carbon cloth has received considerable attention as a potential adsorbent for water treatment applications. Activated carbon cloth has been used for successful adsorptive removal of various inorganic anions (9, 10) and some aromatic organic compounds (11–17). Some metal ions were also reported (18–22) to be effectively adsorbed onto activated carbon cloth. Studies on competitive adsorption from binary mixtures onto activated carbon cloth (23) have proven the potential use of this adsorbent for separation purposes.

The purpose of the present work is to determine the adsorption characteristics of benzaldehyde (BA), sodium salt of p-phenolsulfonic acid (p-PhS) and

sulphanilic acid (SA) in water, in an acidic medium, or in a basic medium onto activated carbon cloth. The investigation of competitive adsorption of these compounds from their binary mixtures was also aimed in order to determine suitable medium for selective removal of the compounds studied.

MATERIALS AND METHODS

Materials

The activated carbon cloth (ACC) used in the present work was obtained from Spectra Corp. (MA, USA) coded as Spectracarb 2225. Although the full details of its mode of preparation are regarded as proprietary, it originates from pyrolysis of phenolic polymer fibers followed by heat treatment in O_2-free N_2 between 800 and 900°C for some hours. In this respect, it differs from other fibrous carbon materials derived by pyrolysis of rayon (11).

Benzaldehyde was obtained from Merck, sulphanilic acid from Panreac, and sodium salt of p-phenolsulfonic acid from Eastman Kodak. All other chemicals were reagent grade. Deionized water was used in adsorption experiments.

Treatment and Properties of the Carbon Cloth

The activated carbon fibers are known to provide spontaneously a small but significant quantity of ions into the conductivity water. These ions are expected to be introduced into the fibers during the activation process (9). The problem of release of undesired ions by porous carbon materials was also reported by Soffer and Folman (24). Therefore a deionization cleaning procedure was applied to avoid desorption of these ions during adsorption studies. This procedure was described in detail in our early works (9, 14, 15).

The specific surface area and porosity of treated carbon cloth were obtained from N_2 adsorption isotherms at -196°C. Prior to N_2 adsorption experiments to determine surface properties, ACC samples were degassed at 130°C under vacuum (up to 10^{-6} torr) for 12 h. The N_2 adsorption data were obtained at the Central Laboratory of Middle East Technical University, Ankara, Turkey, according to the multipoint BET method with a Quantachrome Autosorb-1-C/MS apparatus over a relative pressure ranging from 10^{-6} to 1. The BET specific surface area, total pore volume, micropore volume, mesopore volume, and pore size distribution of ACC were yielded by using the software of the apparatus. The specific surface area of the ACC samples were calculated according to the Brunauer, Emmet, Teller method (25) using the nitrogen adsorption isotherm data given in Fig. 1.

The pore size distribution curve obtained according to Density Functional Theory (DFT) (26) is given in Fig. 2 which shows that the ACC consists of pores mainly in micropore character (< 20 Å). The SEM pictures of treated

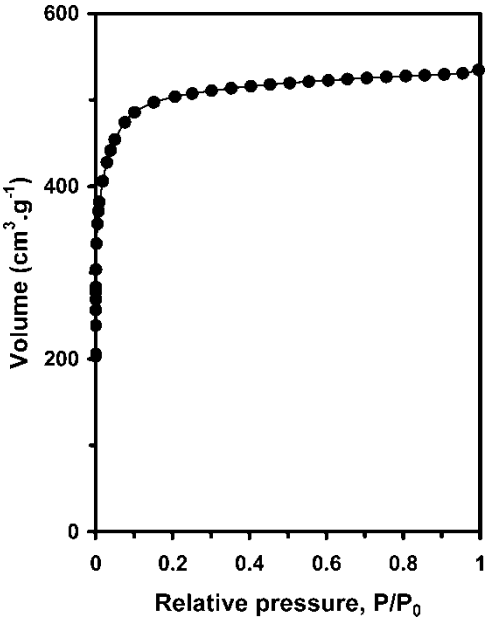

Figure 1. Nitrogen adsorption isotherm of ACC.

(washed) carbon-cloth were previously given (27) from which the average fiber diameter was estimated (15).

The pH_{PZC} of an adsorbent is the pH of a solution containing this adsorbent when the net surface charge is zero. The pH_{PZC} of the activated carbon cloth used in the present study was previously measured (14, 15) in 0.1 M $NaNO_3$, in 0.05 M $NaNO_3$, or 0.01 M $NaNO_3$ by a batch equilibrium method described by Babić et al. (27). The contents of the acidic and basic surface groups on the ACC were determined previously (28) according to the Boehm method (29).

All the properties of treated ACC obtained by the procedures described above are collectively given in Table 1 together with elemental analysis results.

The Design of the Adsorption Cell and Optical Absorbance Measurements

A specially designed cell was used to carry out the adsorption and simultaneously to perform in-situ concentration measurements by means of UV absorption spectrophotometry. This cell was described in detail including a diagram in our previous works (9, 14, 15).

With the use of this adsorption cell it was possible to follow the changes in concentration of the adsorbate solution during the course of adsorption by

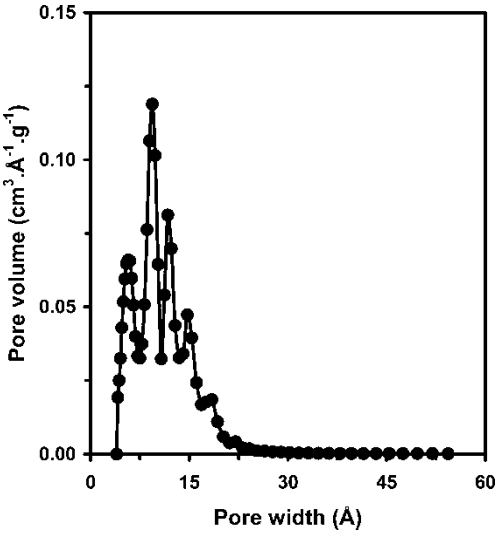

Figure 2. Pore size distribution of treated ACC according to DFT theory.

in-situ uv-spectroscopy. Solutions of adsorbates were prepared in water at natural pH, in 1 M H_2SO_4 or in 0.1 M NaOH to examine the effects of both the surface charge of the carbon cloth and the ionization of adsorbates on adsorption. The initial concentrations of adsorbates and the amount of carbon cloth were kept as constant as possible for kinetic studies of adsorption in order to make an easy comparison (concentration: 1×10^{-4} M, mass of carbon cloth: 15.0 ± 0.1 mg). The carbon-cloth pieces were pre-wetted by

Table 1. Properties of treated activated carbon cloth

Specific surface area	1870 $m^2 \cdot g^{-1}$
Total pore volume	0.827 $cm^3 \cdot g^{-1}$
Micropore volume	0.709 $cm^3 \cdot g^{-1}$
Mesopore volume	0.082 $cm^3 \cdot g^{-1}$
Average fiber diameter	17 μm
Carbon content	95.14 %
Hydrogen content	0.37 %
Oxygen content	4.49 %
Nitrogen and sulfur content	0 %
pH_{PZC}	7.4
Total acidic group content	0.25 mmol $\cdot g^{-1}$
Carboxylic group content	0.093 mmol $\cdot g^{-1}$
Lactonic group content	0.020 mmol $\cdot g^{-1}$
Phenolic group content	0.14 mmol $\cdot g^{-1}$
Total basic group content	0.28 mmol $\cdot g^{-1}$

being left in water for 24 h before use. During this long contact period with water, the pores of the carbon cloth may expand and become more accessible for the adsorbate in the actual adsorption process. The idea of using a pre-wetted carbon cloth originated from our previous findings that pre-wetting enhances the adsorption process (9, 23).

The carbon cloth piece was dipped into the adsorption cell initially containing only water and then a vacuum was applied to remove all air in the pores of the carbon cloth. The wetted and degassed carbon cloth was removed from the cell for a short time and water in the cell was replaced with a known volume of sample solution (20 mL). The sliding door of the sample compartment of the spectrophotometer was left half-open and the quartz cuvette fixed at the bottom of the adsorption cell (which now contained the sample solution) was inserted into the front sample compartment. N_2 gas was passed through the adsorption cell to provide effective mixing. Finally, the carbon cloth, which was removed temporarily after wetting and degassing, was re-inserted into the solution in the adsorption cell. Then, quickly, an opaque curtain was spread above the sample compartment of the spectrophotometer, over the cell, to prevent interference from external light. A Shimadzu 160A UV/VIS spectrophotometer was used for the optical absorbance measurements.

The program for monitoring the absorbance at the specific wavelength of maximum absorbance predetermined by taking the whole spectrum of each adsorbate was then run on the built-in microcomputer of the spectrophotometer. The absorbance data was recorded in programmed time intervals of 1 min over a period of 90 min.

The absorbance data were converted into concentration data using calibration relations pre-determined at the wavelength of maximum absorbance for each adsorbate.

Determination of Adsorption Isotherms

The adsorption isotherms of adsorbates were determined on the basis of batch analysis. The carbon cloth pieces of varying masses were allowed to equilibrate with solutions of adsorbates in 1 M H_2SO_4, in water at natural pH, or in 0.1 M NaOH with known initial concentrations at 30°C for 48 h. Preliminary tests showed that the concentration of adsorbates remained unchanged after a 20–24 h contact with the carbon cloth. So, the allowed contact time of 48 h ensures the equilibration. The equilibration was allowed in 100 mL erlenmeyer flasks kept in Nüve ST 402 shaking water-bath at a constant shaking speed of 150 rpm. The concentrations after the equilibration period were measured spectrophotometrically. The amount of adsorbate adsorbed at equilibrium per unit mass of the carbon cloth, q_e, was calculated by Eq. (1)

$$q_e = \frac{V(C_0 - C_e)}{m} \tag{1}$$

where V is the volume of the solution of adsorbate in L, C_0 and C_e are the initial and equilibrium concentrations, respectively, in mM and m is the mass of carbon cloth in g. Then Eq. (1) gives q_e in mmol adsorbate adsorbed per g carbon cloth.

RESULTS AND DISCUSSION

Chemical Nature, Optical Absorption Characteristics, and Calibration Data of the Adsorbates

The chemical, spectral, and calibration data for the adsorbates studied are given in Table 2. Separate calibration experiments were run to determine the molar absorptivities (ε) required for calibration using aqueous solutions of the pure compounds. Absorbance versus concentration data for each single compound was treated according to the Lambert-Beer law by linear regression analysis to determine ε and the regression coefficient, r.

Adsorption Behaviors of Individual Adsorbates over 90 Min

The concentration versus time plots over an adsorption period of 90 min for all adsorbates (BA, SA, and p-PhS) in water, in 1 M H_2SO_4 and in 0.1 M NaOH is shown in Figs. 3, 4 and 5, respectively. It is clear from these figures that BA is the adsorbate having the highest extent of adsorption among the three adsorbates studied in all three solvents.

In water, the concentration of BA, SA, and p-PhS decreased from 1.01×10^{-4} M to 3.07×10^{-6} M; from 1.02×10^{-4} M to 3.34×10^{-5} M and from 1.00×10^{-4} M to 3.12×10^{-5} M, respectively, over the 90 min adsorption (Fig. 3). These lowerings in concentrations correspond to 97.0%, 67.2%, and 68.8% removal for BA, SA, and p-PhS, respectively. SA and p-PhS show similar adsorption trends. Their extent of adsorption are less than the extent of adsorption of BA. These behaviors can be explained on the basis of interactions between the adsorbates and the adsorbent. Analytical calculations using K_a value showed that SA in water is 87.1% in anionic form (negative charge is on sulfonate group) and 12.9% in zwitterionic form (negative charge is on sulfonate, positive charge is on ammonium group). On the other hand, p-PhS in water was found to be more than 99% in anionic form, the negative charge being on the sulfonate group. The initial pH of solutions of the three adsorbates in water was measured as 4.2, 5.7, and 5.7 for SA, BA, and p-PhS, respectively, and they changed only slightly during the adsorption. The pH values at equilibrium were 4.8, 5.8, and 6.2, respectively. Since the pH_{PZC} of ACC is close to neutral (7.4), surface of the ACC is expected to possess a small positive charge. BA is an unionizable adsorbate in neutral molecular form. Therefore its adsorption by the ACC involves mainly hydrogen bonding and dispersion interactions.

Table 2. Spectral and calibration data for adsorbates

Adsorbate	Molecular structure	Solvent	λ_{max}/ nm	ε/ $M^{-1}cm^{-1}$	r
BA	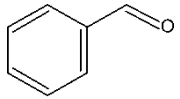	H_2O	250	11080	0.9999
		H_2O	230[a]	4480	0.9993
		0.1 M NaOH	250	11040	0.9994
		1 M H_2SO_4	250	11130	0.9997
		1 M H_2SO_4	215[a]	2190	0.9885
SA	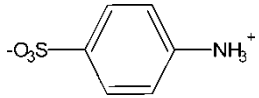	H_2O	249	13500	0.9987
		0.1 M NaOH	249	11040	0.9986
		1 M H_2SO_4	215	8300	0.9991
		1 M H_2SO_4	250[a]	665	0.9903
p-PhS	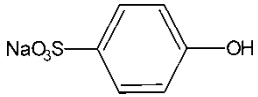	H_2O	230	12300	0.9997
		H_2O	271	986	0.9997
		H_2O	250[a]	630	0.9805
		0.1 M NaOH	254	17400	0.9995
		1 M H_2SO_4	230	11800	0.9970
		1 M H_2SO_4	271	988	0.9955

[a]Not λ_{max}. Determined for the analysis of binary mixtures.

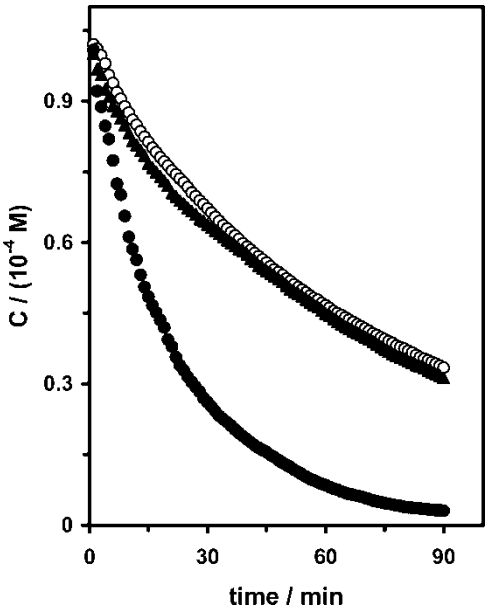

Figure 3. Concentration versus time plots for the adsorption of BA (●), p-PhS (○), and SA (▲) in water.

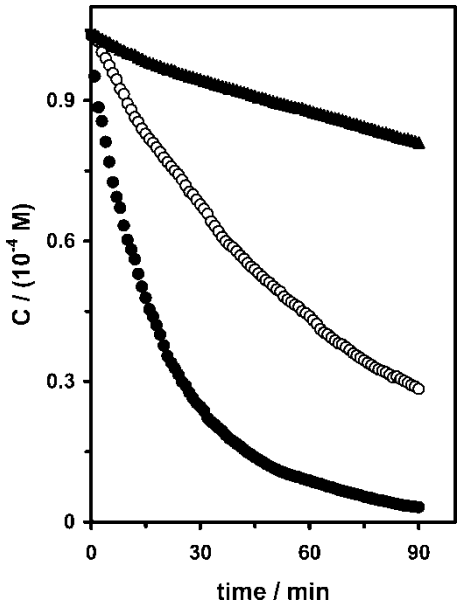

Figure 4. Concentration versus time plots for the adsorption of BA (●), p-PhS (○), and SA (▲) in 1 M H_2SO_4.

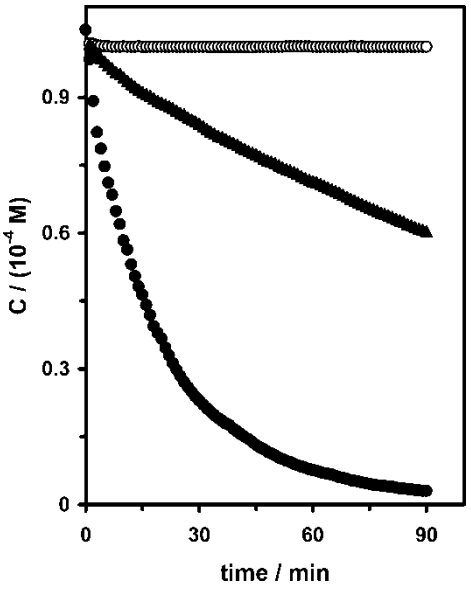

Figure 5. Concentration versus time plots for the adsorption of BA (●), p-PhS (○), and SA (▲) in 0.1 M NaOH.

Both SA and p-PhS have $-SO_3^-$ group in their structure. These groups were found to be weakly adsorbed by ACC; for example in one of our earlier works (9), SO_4^{-2} was found to have a small negative adsorption. Therefore, the finding of smaller extents of adsorption by SA and p-PhS than BA is not surprising. The groups $-OH$ and $-NH_2/NH_3^+$ in para position to SO_3^- in p-PhS and SA, respectively, are expected to be similar in character in making hydrogen bonding with the surface functional groups. The presence of a small amount of $-NH_3^+$ group (only 12.9%) in SA seems not to affect its adsorption in an important way, on the basis of the observation of similar trends in adsorption of p-PhS and SA (Fig. 3).

The adsorption data in 1 M H_2SO_4 given in Fig. 4 shows that the removal percentages of BA, SA and p-PhS in this solvent over 90 min of adsorption are 97.1, 22.9 and 73.1, respectively. ACC surface is positively charged in this medium ($pH < pH_{PZC}$). Calculations have shown that in 1 M H_2SO_4;

i. SA is 25% in zwitterionic form (the negative charge is on sulfonate and the positive charge is on the ammonium group) and 75% in cationic form (positive charge is on the ammonium group; the sulfonate group is neutralized with a proton in this form).
ii. p-PhS is 25% in anionic form (negative charge is on sulfonate) and 75% in neutral form (—OH group can not ionize; the sulfonate group is neutralized with a proton in this form).
iii. BA is in neutral molecular form as it is an unionizable molecule.

The only difference in charge between SA and p-PhS is that in SA there is an extra positive charge on the ammonium group. Therefore SA experiences some repulsion on the ammonium side of the molecule from the positively charged ACC surface. However, it can still be adsorbed to a small extent from the sulfonate side of the molecule through some hydrogen bonding, dispersion, and electrostatic interactions. p-PhS does not see any electrostatic repulsion from the surface. Therefore it is adsorbed onto the ACC at a greater extent than SA as seen in Fig. 4. BA is adsorbed most strongly by the ACC surface through hydrogen bonding and dispersion interactions without any repulsion. Since BA has no para substituent its phenyl group is probably approaching more to surface resulting in more π-π dispersion interactions.

In 0.1 M NaOH solution, p-PhS is almost not adsorbed on the ACC (Fig. 5). At the end of 90 min its removal percentage is only 0.98. This can be explained with the surface charge of ACC in 0.1 M NaOH and the structure of the p-PhS. The surface of the carbon cloth is negatively charged ($pH > pH_{PZC}$) and p-PhS has two negatively charged groups ($-SO_3^-$ and O^-) in 0.1 M NaOH. Thus electrostatic repulsions between the adsorbate and the adsorbent predominate resulting in negligible adsorption under these conditions. The removal percentage of SA is 40.9% in 0.1 M NaOH over 90 min. This removal percentage for SA is intermediate between the other two adsorbates, p-PhS and BA (Fig. 5). Analytical calculations have shown that in 0.1 M NaOH, SA is in anionic form with a single negative charge on the sulfonate group. This means that it has one less negative charge than p-PhS, thus it experiences less repulsion from the negatively charged ACC surface than p-PhS. This explains the higher extent of adsorption observed for SA than p-PhS in Fig. 5. On the other hand, BA is still in neutral molecular form in 0.1 M NaOH as it was in water and 1 M H_2SO_4 since it is an unionizable compound. So, it experiences no electrostatic repulsion from the negatively charged ACC surface, resulting in the highest extent of adsorption among the three adsorbates as seen in Fig. 5 due to its hydrogen bonding and dispersion interactions with the surface. The removal percentage of BA after 90 min of adsorption was found to be 97.1.

The adsorption data over a 90 min period were treated according to the first order kinetics by plotting ln $[C_0/C_t]$ as a function of time, t, and applying linear regression analysis according to the following equation:

$$\ln[C_0/C_t] = kt \tag{2}$$

where C_0 and C_t are the initial concentration and the concentration at any time of the adsorbates, respectively, and k is the rate constant. The rate constants were determined from the slope. The rate constants and the regression coefficients obtained by this treatment are given in Table 3. Closeness of regression coefficients to 1 (> 0.99) supports the assumption of the first order rate for the

Table 3. First order rate constants and regression coefficients for the adsorption of studied compounds

Adsorbate	Solvent	k/min^{-1}	r
BA	H_2O	0.0423	0.9940
	1 M H_2SO_4	0.0415	0.9857
	0.1 M NaOH	0.0428	0.9867
SA	H_2O	0.0135	0.9928
	1 M H_2SO_4	0.0030	0.9870
	0.1 M NaOH	0.0060	0.9964
p-PhS	H_2O	0.0131	0.9955
	1 M H_2SO_4	0.0186	0.9983
	0.1 M NaOH	–	–

adsorption process. The order of rate of adsorption of the three adsorbates as indicated by the rate constants is BA > SA ≈ p-PhS in water, BA > p-PhS > SA in 1 M H_2SO_4, and BA > SA >> p-PhS in 0.1 M NaOH.

Competitive Adsorption

Kinetic results presented in Figs. 3–5 show that the adsorption behaviors of the three adsorbates are quite different. This fact can be utilized in selective adsorption of individual adsorbates from mixtures for separation purposes. The in-situ UV-spectroscopic method used in this study allows monitoring the simultaneous adsorption of two or more components from mixtures provided that the components have different optical absorbance maxima. The concentration of each component in a mixture of two species, X and Y, each obeying the Lambert-Beer law, can be determined by simultaneous solution of Eqs. (3) and (4),

$$A(\text{at } \lambda_1) = \varepsilon_X(\text{at } \lambda_1) \cdot C_X + \varepsilon_Y(\text{at } \lambda_1) \cdot C_Y \quad (3)$$

$$A(\text{at } \lambda_2) = \varepsilon_X(\text{at } \lambda_2) \cdot C_X + \varepsilon_Y(\text{at } \lambda_2) \cdot C_Y \quad (4)$$

where A is the absorbance, λ_1 and λ_2 are the wavelengths of the absorption bands, ε_X and ε_Y are the molar absorptivities and C_X and C_Y are the concentrations of X and Y, respectively. The light pathlength, being 1 cm, does not appear in Eqs. (3) and (4). Solutions of these equations require molar absorptivities of each component at the two wavelengths determined separately with solutions of the respective pure components.

As an application, two example binary mixtures were chosen and competitive adsorption of its components was followed. The selected systems were equimolar mixture of BA and SA in 1 M H_2SO_4 and of BA and p-PhS

in H_2O. The adsorption was followed at the wavelengths of 215 and 250 nm for BA-SA mixture in 1 M H_2SO_4 and of 230 and 250 nm for BA-p-PhS in H_2O. The required ε values are given in Table 2.

The results of the competitive adsorption are given below for the two selected systems separately.

Equimolar Mixture of BA and SA in 1 M H_2SO_4

Concentration versus time plot for the competitive adsorption of BA and SA in 1 M H_2SO_4 is shown in Fig. 6 where corresponding plots for adsorption from solutions of individual components are also shown for comparison. It is clear that an important degree of separation is achieved at the end of 90 min. The adsorption behavior of BA from the mixture is almost the same as that from its individual solution. The adsorption behavior of SA from the mixture is again almost the same as that from its individual solution for the first 45 min, but after that the rate of its adsorption from the mixture is almost diminishing while its adsorption from individual solution continues almost at the same rate. This difference in adsorption behavior of SA helps the separation of the two components from this mixture.

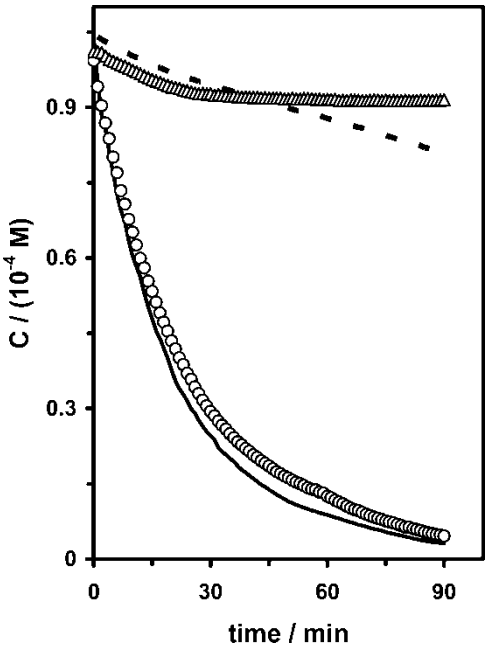

Figure 6. Adsorption of BA and SA from equimolar mixtures and from individual solutions in 1 M H_2SO_4. (○): BA from mixture, (△): SA from mixture, (——): BA from its individual solution, and (. . .): SA from its individual solution.

Equimolar Mixture of BA and p-PhS in Water

Concentration versus time plot for the competitive adsorption of BA and p-PhS in water is given in Fig. 7 where the corresponding plots for adsorption from individual solutions are also shown for comparison. Although it is not as much as in the case of BA-SA system in 1 M H_2SO_4, a certain degree of separation is achieved at the end of 90 min adsorption period. The extent of adsorption of both components from equimolar mixture decrease considerably compared to those from individual solutions. This may result from two factors. The total amount of adsorbate in the mixture is twice that of in the individual solutions. Thus, a decrease in adsorption of each component from the mixture compared to that from individual solutions is expected considering the limited adsorption capacity of the ACC. Secondly, BA and p-PhS in water may interact with each other through intermolecular hydrogen bonding, ion-dipole, or dipole-dipole interactions in such a way that their adsorption centers may be blocked.

Adsorption Isotherms

Adsorption isotherm data were derived with batch analysis at 30°C. The isotherm data were treated according to two well known isotherm equations;

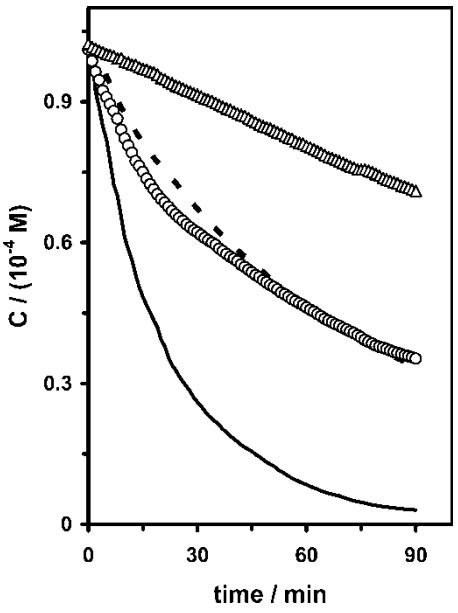

Figure 7. Adsorption of BA and p-PhS from equimolar mixtures and from individual solutions in water. (○): BA from mixture, (△): p-PhS from mixture, (——): BA from its individual solution, and (. . .): p-PhS from its individual solution.

Langmuir and Freundlich. The linearized forms of Langmuir and Freundlich isotherm equations are given in Eqs. (5) and (6), respectively (30, 31);

$$\frac{C_e}{q_e} = \frac{C_e}{q_{max}} + \frac{1}{b\ q_{max}} \tag{5}$$

$$\ln q_e = \ln K_F + (1/n) \ln C_e \tag{6}$$

where q_e is the amount of adsorbate adsorbed per unit mass of adsorbent at equilibrium in $mmol \cdot g^{-1}$, C_e is the final concentration at equilibrium in mM, q_{max} is the maximum adsorption at monolayer coverage in $mmol \cdot g^{-1}$, b is the adsorption equilibrium constant related to the energy of adsorption in mM^{-1}, K_F is the Freundlich constant representing the adsorption capacity in $(mmol \cdot g^{-1})\ (mM^{-1})^{1/n}$ and n is a constant related to surface heterogeneity.

Parameters of Langmuir and Freundlich isotherm equations and regression coefficients (r) for the adsorbates studied are given in Table 4. The isotherms predicted with these parameters for adsorbates in water, in 1 M H_2SO_4 and 0.1 M NaOH are presented in Figs. 8–10, respectively, together with the experimental data points.

As can be seen from Table 4, the regression coefficients of the Langmuir model are generally lower than those of the Freundlich model, except for adsorption of SA in H_2O and in 1 M H_2SO_4. This shows that the fit of the experimental data to the Freundlich model is generally better than the Langmuir model.

A better criterion for the assessment of experimental isotherm data is a parameter known as normalized percent deviation (32) or in some literature as percent relative deviation modulus, P, (33, 34) given by the following equation

$$P = \frac{100}{N} \sum_{i=1}^{N} \frac{\left| q_{e(\text{pred})} - q_{e(\text{exp})} \right|}{q_{e(\text{exp})}} \tag{7}$$

where $q_{e\ (expt)}$ is the experimental q_e at any C_e, $q_{e\ (pred)}$ is the corresponding predicted q_e according to the equation under study with the best fitted parameters and N is the number of experimental data points. It is clear that the lower the P value, the better is the fit. The P values calculated for each set of isotherm data given in Table 4, are lower for the Freundlich model than for Langmuir model with the only exception of the system of SA in 0.1 M NaOH. So, the results of analysis on the basis of P values support the conclusion reached on the basis of regression coefficients.

The Freundlich parameter, K_F, which is an indicator of the adsorption capacity, increases in the order of p-PhS < SA < BA in water and in 0.1 M NaOH and in the order of SA < p-PhS < BA in 1 M H_2SO_4 (Table 4). Also according to the K_F parameters given in Table 4, the order of adsorption capacity of ACC in different solvents is water $\approx$ 1 M H_2SO_4 < 0.1 M NaOH for BA; 1 M H_2SO_4 < 0.1 M NaOH < water for SA and 0.1 M NaOH < water < 1 M H_2SO_4 for p-PhS.

Table 4. Parameters of Langmuir and Freundlich isotherm equations, regression coefficients (r) and normalized percent deviation (P) for adsorbates studied at 30°C

		Langmuir parameters				Freundlich parameters			
Adsorbate	Solvent	q_{max} ($mmol \cdot g^{-1}$)	b (mM^{-1})	r	P	K_F ($mmol \cdot g^{-1}$) $\cdot$ (mM^{-1})$^{1/n}$	1/n	r	P
BA	H_2O	2.80	49.9	0.9897	12.7	4.90	0.337	0.9952	2.71
	1 M H_2SO_4	2.71	22.9	0.9757	9.78	4.41	0.398	0.9948	2.74
	0.1 M NaOH	3.16	35.8	0.9943	6.22	6.68	0.427	0.9946	3.28
SA	H_2O	0.550	26.4	0.9829	4.81	0.843	0.331	0.9717	3.49
	1 M H_2SO_4	0.029	42.8	0.9717	1.33	0.048	0.299	0.8749	1.30
	0.1 M NaOH	0.128	9.29	0.9567	1.15	0.347	0.716	0.9926	1.25
p-PhS	H_2O	0.301	20.1	0.9936	1.45	0.516	0.407	0.9946	1.05
	1 M H_2SO_4	0.819	18.2	0.9932	2.03	1.45	0.441	0.9968	0.904
	0.1 M NaOH	–	–	–	–	–	–	–	–

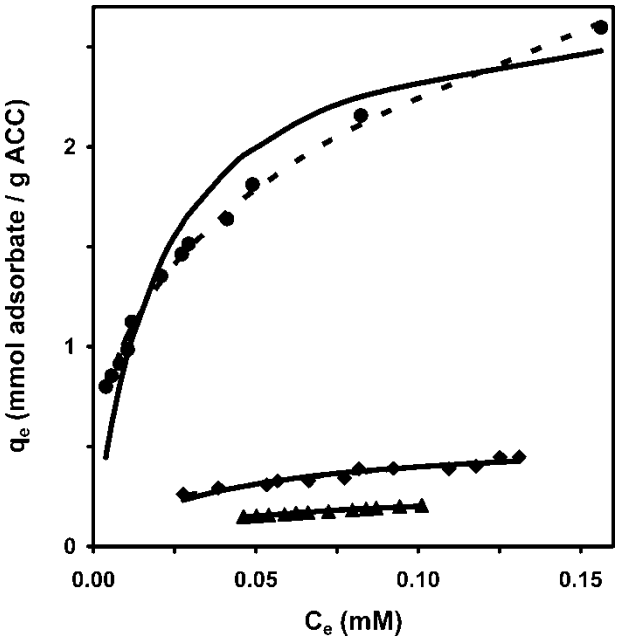

Figure 8. Adsorption isotherm data of BA (●), SA (◆), and p-PhS (▲) in water. Langmuir model (——), Freundlich model (···).

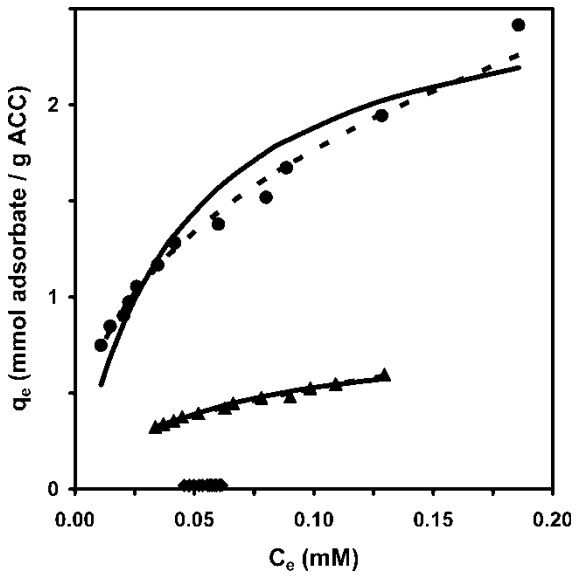

Figure 9. Adsorption isotherm data of BA (●), SA (◆), and p-PhS (▲) in 1 M H_2SO_4. Langmuir model (——), Freundlich model (···).

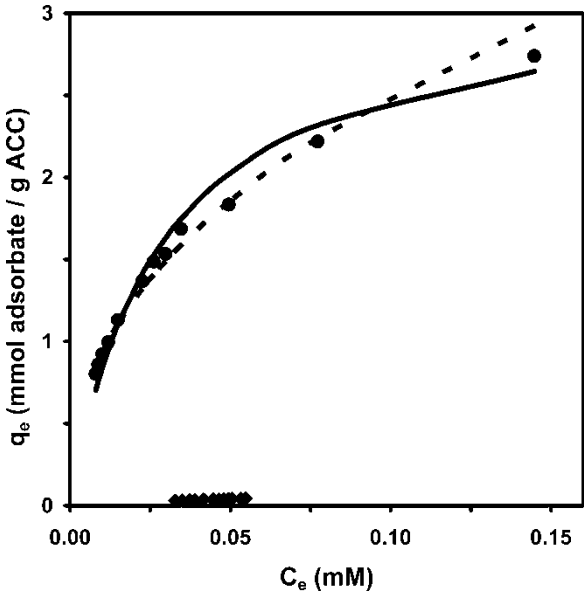

Figure 10. Adsorption isotherm data of BA (●), and SA (◆) in 0.1 M NaOH. Langmuir model (——), Freundlich model (· · ·).

CONCLUSIONS

Removal of BA, SA, and p-PhS from aqueous solution is achieved to a considerable extent by adsorption onto ACC and this can be followed by in-situ UV-spectroscopy. The adsorption medium (water, 0.1 M NaOH, or 1 M H_2SO_4) may alter the adsorption characteristics and trends of BA, SA, and p-PhS. The most striking alteration was with p-PhS which became almost unadsorbable in 0.1 M NaOH while it was adsorbed in H_2O or 1 M H_2SO_4 to a considerable extent. The separation of SA and BA from equimolar mixture to a considerable extent and of BA and p-PhS again from equimolar mixture to a certain extent was found to be possible by adsorption onto ACC. Kinetic data over 90 min adsorption for SA, BA, and p-PhS fitted successfully to first order law. The Freundlich isotherm model represented the experimental isotherm data better than the Langmuir model.

ACKNOWLEDGEMENTS

The authors would like to thank the Scientific Research Projects Unit of Akdeniz University for support of this work through project 2003.01.0300.009 and to the central laboratory of METU (Middle East Technical University) for determining the surface properties of ACC.

REFERENCES

1. Howe-Grant, M. (1992) *Kirk-Othmer Encyclopedia of Chemical Technology*; John Wiley & Sons: New York; Vol. 4.
2. Radovic, L.R., Silva, I.F., Ume, J.I., Menendez, J.A., Leon-Leon, C.A., and Scaroni, A.W. (1997) An experimental and theoretical study of the adsorption of aromatics possessing electron-withdrawing and electron-donating functional groups by chemically modified activated carbons. *Carbon*, 35: 1339.
3. Sakoda, A., Suzuki, M., Hirai, R., and Kawazoe, K. (1991) Trihalomethane adsorption on activated carbon fibers. *Water Research*, 25: 219.
4. Grajek, H., Neffe, S., and Witkiewicz, Z. (1992) Chromatographic determination of the physico-chemical parameters of adsorption on activated carbon fibres. *Journal of Chromatography*, 600: 67.
5. Miyake, Y. and Suzuki, M. (1993) Removal of trichloroethylene from air stripping off-gas by adsorption on activated carbon fibre. *Gas Separation & Purification*, 7: 229.
6. Jaroniec, M., Madey, R., Choma, J., McEnaney, B., and Mays, T.J. (1989) Comparison of adsorption methods for characterizing the microporosity of activated carbons. *Carbon*, 27: 77.
7. Dabrowski, A. (2001) Adsorption-from theory to practice. *Advances in Colloids and Interface Science*, 93: 135.
8. D'Silva, A.P. (1998) Adsorption of antioxidants by carbon blacks. *Carbon*, 36: 1317.
9. Ayranci, E. and Conway, B.E. (2001) Adsorption and electrosorption at high-area carbon felt electrodes for waste-water purification: systems evaluation with inorganic, S-containing anion. *Journal of Applied Electrochemistry*, 31: 257.
10. Afkhami, A. (2003) Adsorption and electrosorption of nitrate and nitrite on high-area carbon cloth: an approach to purification of water and waste-water samples. *Carbon*, 41: 1309.
11. Ayranci, E. and Conway, B.E. (2001) Removal of phenol, phenoxide and chlorophenols from waste-waters by adsorption and electrosorption at high-area carbon felt electrodes. *Journal of Electroanalytical Chemistry*, 513: 100.
12. Duman, O. and Ayranci, E. (2004) Removal of phenol, p-cresol and p-nitrophenol from aqueous solutions by adsorption at high-area activated carbon cloth, In Proceedings of 4th Aegean Analytical Chemistry Days, Kuşadası, Turkey, pp. 566–568.
13. Duman, O. and Ayranci, E. (2004) Adsorption of aniline and its derivatives from aqueous solutions onto activated carbon cloth studied by in-situ uv spectroscopy. In Proceedings of 4th Aegean Analytical Chemistry Days, Kuşadası, Turkey, pp. 402–404.
14. Duman, O. and Ayranci, E. (2005) Structural and ionization effects on the adsorption behaviors of some anilinic compounds from aqueous solution onto high-area carbon cloth. *Journal of Hazardous Materials*, B120: 173.
15. Ayranci, E. and Duman, O. (2005) Adsorption behaviors of some phenolic compounds onto high specific area activated carbon cloth. *Journal of Hazardous Materials*, B124: 125.
16. Pignon, H., Faur-Brasquet, C., and Le Cloirec, P. (2000) Treatment of complex aqueous solutions by the coupling of ultrafiltration and adsorption onto activated carbon cloth. *Environmental Technology*, 21: 1261.
17. Brasquet, C., Bourges, B., and Le Cloirec, P. (1999) Quantitative structure-property relationship (QSPR) for the adsorption of organic compounds onto

activated carbon cloth: Comparison between multiple linear regression and neutral network. *Environmental Science and Technology*, 33: 4226.
18. Faur-Brasquet, C., Kadirvelu, K., and Le Cloirec, P. (2002) Removal of metal ions from aqueous solution by adsorption onto activated carbon cloths: adsorption competition with organic matter. *Carbon*, 40: 2387.
19. Kadirvelu, K., Faur-Brasquet, C., and Le Cloirec, P. (2000) Removal of Cu(II), Pb(II), and Ni(II) by adsorption onto activated carbon cloths. *Langmuir*, 16: 8404.
20. Babic, B.M., Milonjic, S.K., Polovina, M.J., Cupic, S., and Kaludjerovic, B.V. (2002) Adsorption of zinc, cadmium, and mercury ions from aqueous solutions on an activated carbon cloth. *Carbon*, 40: 1109.
21. Afkhami, A. and Conway, B.E. (2002) Investigation of removal of Cr(VI), Mo(VI), W(VI), V(IV), and V(V) oxy-ions from industrial waste-waters by adsorption and electrosorption at high-area carbon cloth. *Journal of Colloid and Interface Science*, 251: 248.
22. Rangel-Mendez, J.R. and Streat, M. (2002) Adsorption of cadmium by activated carbon cloth: influence of surface oxidation and solution pH. *Water Research*, 36: 1244.
23. Ayranci, E. and Conway, B.E. (2001) Adsorption and electrosorption of ethyl xanthate and thiocyanate anions at high-area carbon-cloth electrodes studied by in situ UV spectroscopy: development of procedures for wastewater purification. *Anal. Chem.*, 73: 1181.
24. Soffer, A. and Folman, M. (1972) Electrical double-layer of high surface porous carbon electrode. *Journal of Electroanalytical Chemistry*, 38: 25.
25. Brunauer, S., Emmet, P.H., and Teller, E. (1938) Adsorption of gases in multimolecular layers. *Journal of American Chemical Society*, 60: 309.
26. Seaton, N.A., Walton, J.P.R.B., and Quirke, N. (1989) New analysis method for the determination of the pore size distribution of porous carbons from nitrogen adsorption measurements. *Carbon*, 27: 853.
27. Babić, B.M., Milonjić, S.K., Polovina, M.J., and Kaludierović, B.V. (1999) Point of zero charge and intrinsic equilibrium constants of activated carbon cloth. *Carbon*, 37: 477.
28. Ayranci, E. and Duman, O. (2006) Adsorption of aromatic organic acids onto high area activated carbon cloth in relation to waste-water purification. *Journal of Hazardous Materials*, 136: 542.
29. Boehm, H.P. (1966) In *Advances in Catalysis*; Academic press: New York; Vol. 16.
30. Smith, J.M. (1981) *Chemical Engineering Kinetics*; McGraw-Hill: New York.
31. Freundlich, H. and Heller, W. (1939) The adsorption of cis- and trans-azobenzene. *J. Amer. Chem. Soc.*, 61: 2228.
32. Juang, R.-S., Tseng, R.-L., Wu, F.-C., and Lee, S.-H. (1996) Liquid-phase adsorption of phenol and its derivatives on activated carbon fibers. *Separ. Sci. Technol.*, 31: 1915.
33. Lomauro, C.J., Bakshi, A.S., and Labuza, T.P. (1985) Evaluation of food moisture sorption isotherm equations, Part I: fruit, vegetable and meat products. *Lebensm-Wiss. Technol*, 18: 111.
34. Ayranci, E. and Duman, O. (2005) Moisture sorption isotherms of cowpea (Vigna unguiculata L. Walp) and its protein isolate at 10, 20, and 30°C. *J. Food Eng*, 70: 83.